FINE SCALE MODELLING OF CUMULUS CONVECTION

by Terry L. Clark

National Center for Atmospheric Research [1]
Boulder, Colorado 80307

1. INTRODUCTION

Cloud modellers have used two rather different experimental frameworks. In the first framework, the governing equations are solved as an initial value problem without any external forcing to study the evolution of cumulus through to cumulonimbus clouds (Miller, 1978; Wilhelmson and Klemp, 1978; Schlesinger, 1978; Clark, 1979; among others). In this framework an initial region of buoyant air or perhaps circulation is employed to initiate convection. One of the underlying assumptions is that the convection draws its energy from the mean state. The convective available potential energy is usually positive and sufficient to produce a deep cloud and frequently the mean wind shear is such as to allow the development of long lasting severe storms. The initial conditions are rather arbitrary and at times give rise to such effects as storm splitting (Clark,1979). This type of framework, where one models an isolated cloud with a remote environment, has proven useful in understanding certain aspects about the internal dynamics of convective clouds but is of rather questionable use for purposes of studying the dynamics of cloud populations and how they interact with the larger scale flow. There is also some question as to whether or not the unforced initial condition problem is capable of realistically describing certain aspects of the dynamics of cumulus and even multi-cellular severe convective storms. Upshear cumulus development (Clark et al., 1986) and discrete propagation associated with thermally forced waves (Balaji and Clark, 1988) appear to require that cloud modelling be treated more as a forced problem where there is a field of convection. The second experimental framework for modelling clouds is the initial boundary condition approach with external forcing. This approach parallels the approach used in boundary layer modelling where clouds evolve as a result of sensible and latent heating plus some level of excitation (Hill, 1974,1977; Yau and Michaud, 1982; Clark et al. 1986; Balaji

[1] The National Center for Atmospheric Research is sponsored by the National Science Foundation

and Clark, 1988; among others). In this second approach the cloud is part of a field solution where the concept of an isolated cloud with a remote environment is rather obscure. The horizontal scale separation of the clouds is not determined by the initial conditions as specified by the modeller but by the dominant modes of the forced system or by the slowest decaying modes (Ley and Peltier, 1981).

It is this second modelling framework that considers thermal forcing which will be the focus of this workshop paper. The dynamic role of gravity waves in cumulus cloud population studies will be emphasized. In these type of population studies it is usually necessary to use either cyclic boundary conditions to stay in the *near field* of forcing or to use a large enough horizontal domain to allow sufficient time for the convection to attain some sort of Lagrangian equilibrium. Open boundary conditions are a particular problem not so much because of reflection/transmission issues but because the typical inflow boundary data contains no information about the convection activity. Thus, it takes a certain fetch (or Lagrangian time) before the convection can become established after air enteres the domain. The emphasis in this paper will be on mechanistic aspects of the convection rather than upon any detailed statistical anaylsis as in, for example, Xu and Krueger (1991).

2. SIMULATIONS OF NON–PRECIPITATING CUMULUS

i) Two–dimensional dry convection simulations: nonlinear cases

It is instructive to first consider numerical simulations without moisture effects in order to assess the role of the dominant forced modes of the environment on the convection dynamics. Two cases of thermally forced convection were treated by Clark et al. (1986) in two–dimensional space. These cases were derived from the observations of Kuettner et al. (1987). Fig. 1 shows the vertical profiles of $V(z)$, $T(z)$ and $q_v(z)$ used in their studies. q_v is set to zero for the dry runs. The shear spanning the top of the boundary layer and overlying free atmosphere is an important parameter coupling the boundary layer and free atmosphere (Mason and Sykes, 1982). Boundary layer eddies which penetrate into the stable atmosphere through this shear layer exert a drag on the mean flow and excite gravity waves. As a result of the possible effects of wave reflection, trapping, dissipation as well as effects due to variations in phase and

group velocities each horizontal wave number will have a different growth (or decay) rate. Continued thermal forcing will then result in the modes with the slowest decay rates dominating the scale selection.

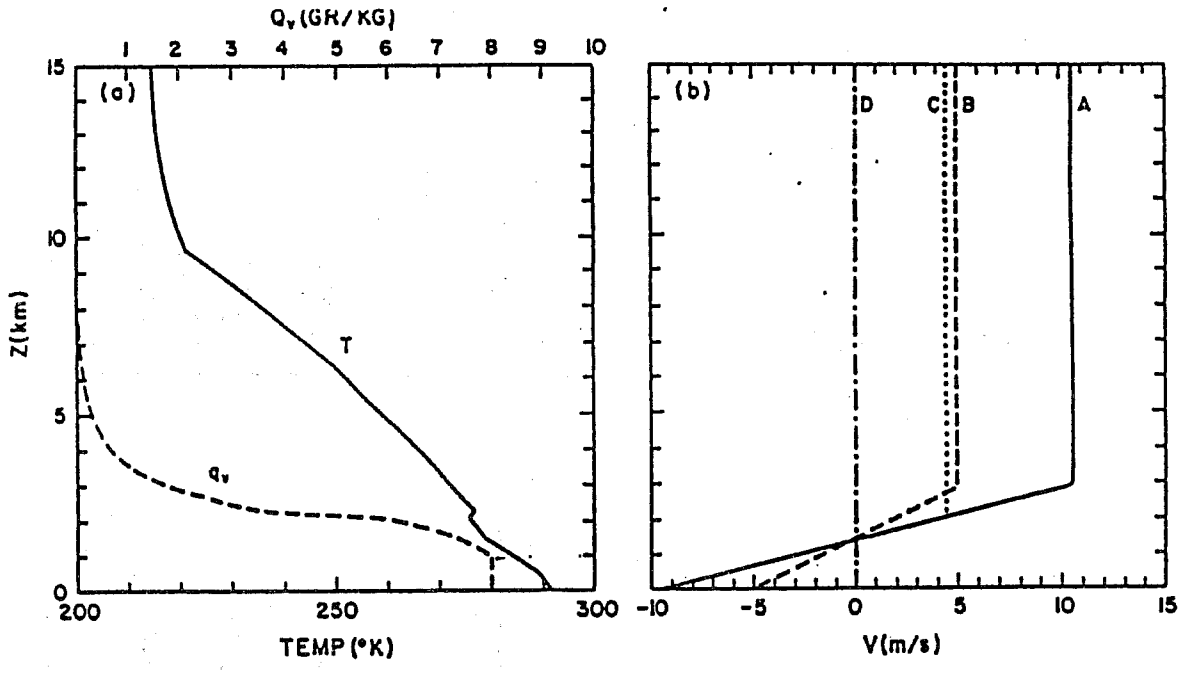

Fig. 1 Environmental profiles of temperature, T, and water vapour, q_v, are shown in (a). Four profiles of environment winds are shown in (b). Profiles of A and B correspond to the strong ($7 \times 10^{-3} s^{-1}$) and moderate ($3.5 \times 10^{-3}\ s^{-1}$) shear cases respectively. (From Clark et al., 1986).

The simulations were forced with the spatially and temporally constant sensible heat flux of 140 Wm^{-2} at z=0. A small random perturbation was added (5% level) as excitation. Figs. 2 and 3 show the results of simulations using shears through the first 2.86 km of depth, of 7.0 and 3.5 $\cdot 10^{-3} s^{-1}$, respectively. At about one hour into the simulations the solutions exhibit gravity waves of significant amplitude. The gravity waves appearing in the stable atmosphere show a narrow range of horizontal scales for the strong shear case and a somewhat broader range of horizontal scales for the moderate shear case. There is also a noticeable difference between the vertical wavelength selection between these two cases.

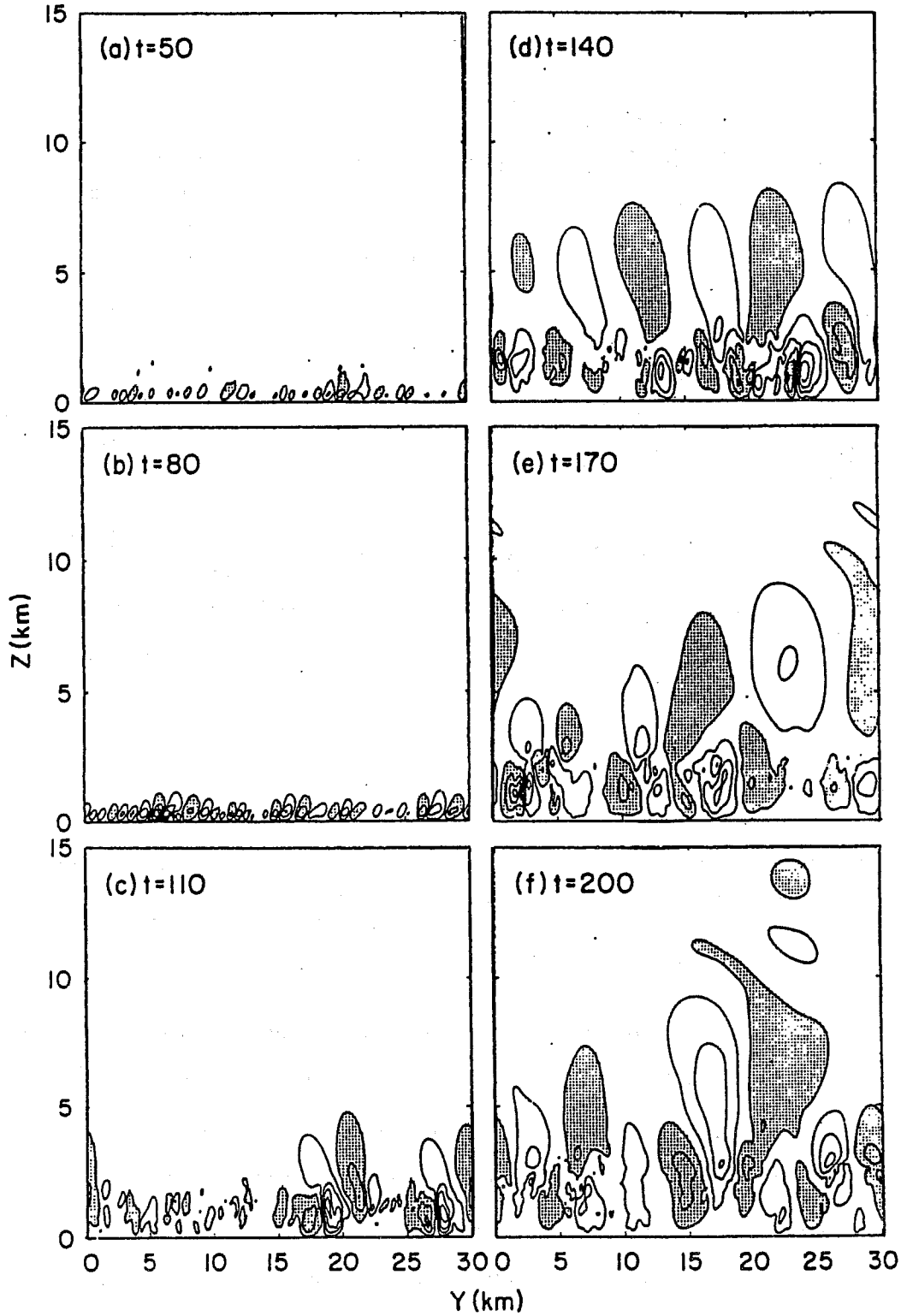

Fig. 2 Six time levels of w. Strong shear case for the dry simulation of Clark et al. (1986). Contour interval is .005 (a), .125 (b) and 1 m s^{-1} (c) through (f). Only odd valued contours are shown and zero contour is not shown.

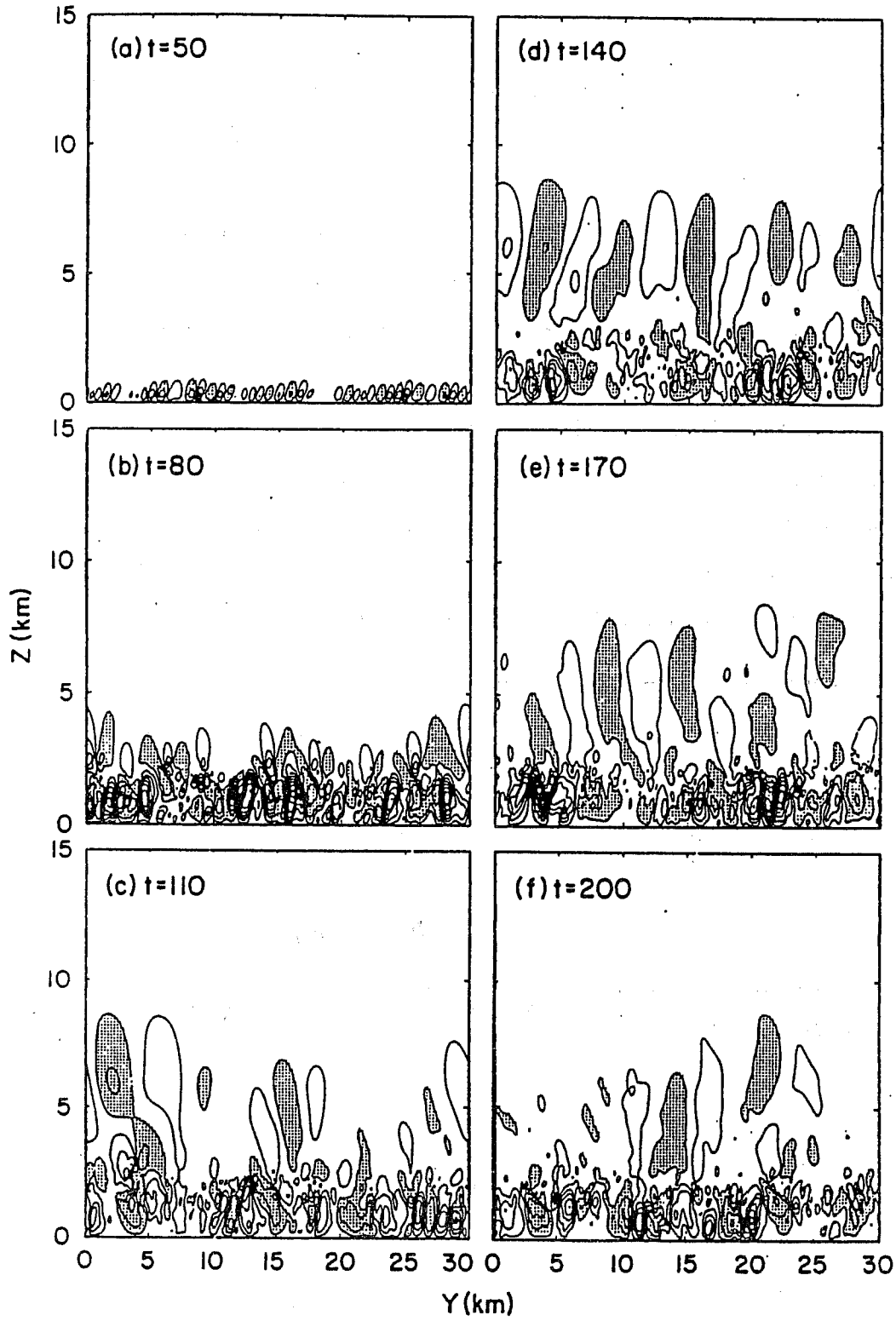

Fig. 3 As in Fig. 2 except for the moderate shear case fro the dry simulation of Clark et al. (1986). Contour interval is .25 (a) and .5 m s^{-1} for plates (b) through (f).

ii) Two-dimensional dry convection simulations: linear cases

To better understand the source of these waves and their scale selection Clark and Hauf (1986) ran the same two cases through a time–dependent linear spectral model. The details of the linear model are presented in Balaji and Clark (1988). Figs. 4 and 5 show the steady–state results from the linear model for the same two shear cases treated by Clark et al. (1986). Fig. 4 shows the power spectra in terms of a one–dimensional energy spectra and also in terms of their vertical structure. The strong shear case shows a distinct peak at $k = 6$ or $\lambda_x = 7.5$ km and a reduced peak at $k = 4$ or $\lambda_x = 11.25$ km. The contour plots of energy against k and z (constant increments of energy) only shows the $k = 6$ structure which is a deep mode extending through to about 8 km. The power spectra for the moderate shear case shows much less dominance by the low wavenumber components and nearly equal amplitude peaks for $k = 5, 8, 10, 16$ corresponding to $\lambda_z = 9$, 5.6, 4.5, 2.8 km.

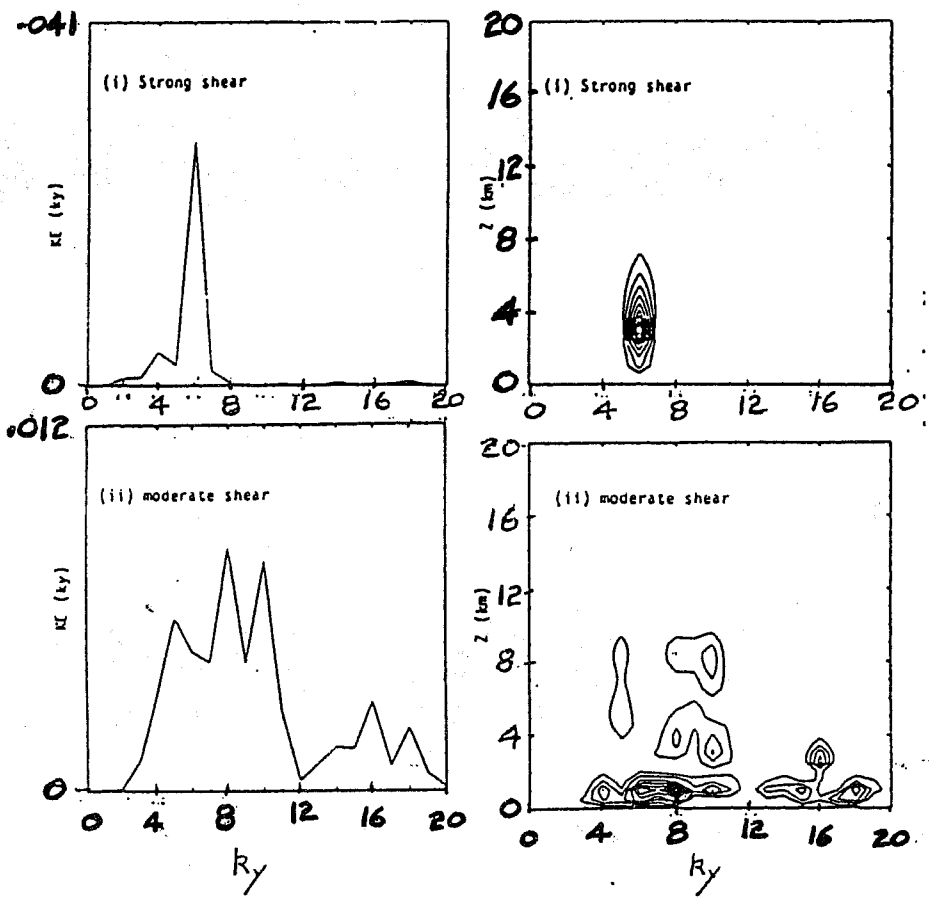

Fig. 4 Power spectra of w from strong and moderate shear cases of Clark et al. (1986) using linear model. Wavenumber k_y=1 corresponds to λ_y = 45 km. Constant contour intervals are used in the $k_y - z$ plots.

The first three of these peaks are deep modes whereas the third appears to be a mode confined to the shear region above the boundary layer. Also evident are the eddies confined to the boundary layer. Fig. 5 shows the two fields of w for the two linear model runs. The fields from both the strong and moderate shear cases from the linear model are similar to those from the full nonlinear simulations.

The deep modes analyzed to date tend to propagate upstream. This propagation sense is most likely a result of efficient coupling between the gravity waves and boundary layer eddies which constitute the full vertical structure of the deep modes.

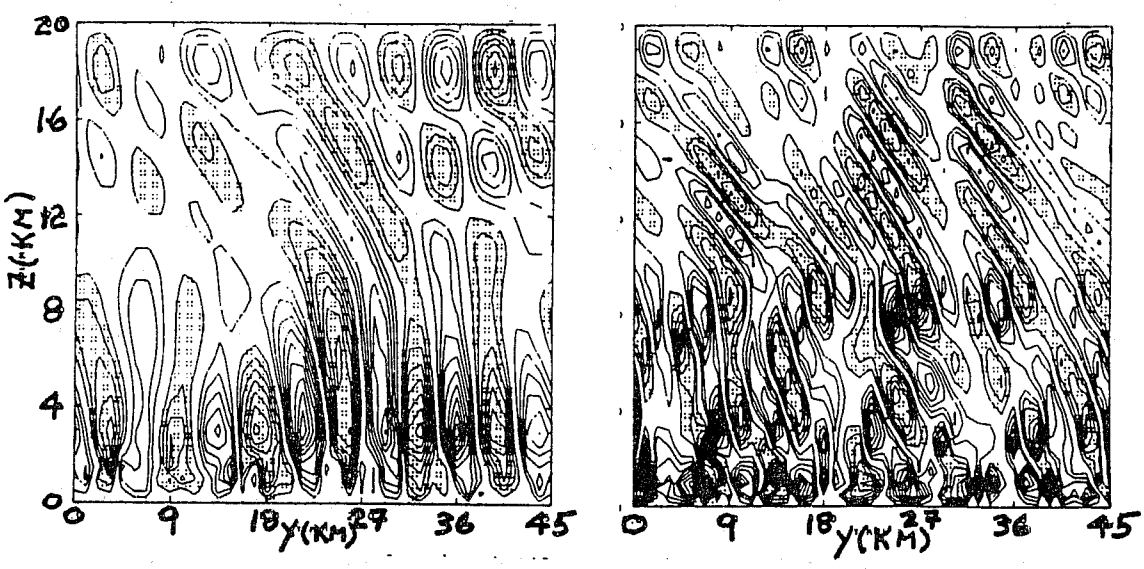

Fig. 5 Fields of w for the strong and moderate shear cases from the linear model whose power spectra were shown in Fig. 4.

These results, then, strongly suggest that for these thermally forced cases the initial horizontal scale selection for the deep modes in the nonlinear model is predictable in terms of the dominant linear forced mode. The linear model predicts similar horizontal scales and shows similar sensitivity to the environmental profiles as the nonlinear model. The initial onset of the deep modes agrees reasonably well with the calculated group velocities, c_g. For the two shear cases $c_g \approx 5$ m s^{-1} which means it takes about 60 min for the wave energy to reach the tropopause and travel back to the top of the boundary layer. This time scale agrees with that occurring in the

nonlinear model where the deep modes begin to appear at about $t > 80$ - 120 min. If the results are explicable in terms of the dominant forced linear modes then one should expect the results to be relatively insensitive to the precise level of excitation used in the thermal forcing or to its horizontal structure. The amplitude of the deep mode response should also scale linearly with the amplitude of the mean thermal forcing.

iii) An inherent nonlinearity of full system

In order to obtain the above degree of comparison between the linear and nonlinear simulations of dry convection with overlying gravity waves it was necessary to excite the linear model with white noise. However, the nonlinear model is forced with a horizontally uniform sensible heat flux with only minor excitation. The sensible heat flux goes directly into horizontally uniform surface values of superadiabatic θ'. Subsequently, perturbations of w at the wavenumber k within the boundary layer interact nonlinearly with θ' to produce θ' values at the wavenumbers k.

iv) Two-dimensional moist convection

The same two cases of shear (Fig. 1) were used with moisture effects turned on. In this case shallow Cu developed as a response to the deep mode updrafts. As already demonstrated the character of the dominant modes for the dry cases was significantly different between the strong and moderate shear cases and one might expect a similar difference with clouds provided of course the clouds are not so energetic so as to over shadow any dominant mode effects. Figs. 6 and 7 show the nature of the cumulus resulting from the strong and moderate shear cases, respectively. Some points to note are that the character of the deep dominant forced modes in the strong shear case (Fig. 6) which give rise to steady boundary layer roots tied to the Cu allowing them to persist and/or develop further with time. The phase of the wave field relative to the eddies appears to determine the character of the clouds. For example, upshear cumulus development appears to be a result of new cloud forming in gravity wave updrafts tied to boundary layer eddies which later merge with existing clouds. The moderate shear case (Fig. 7) has rather transient roots with the waves and eddies tied to each other but propagating right through the clouds. This is a very different cloud field from the previous one and these differences appear to be explicable in terms of the character of the dry dominant forced modes.

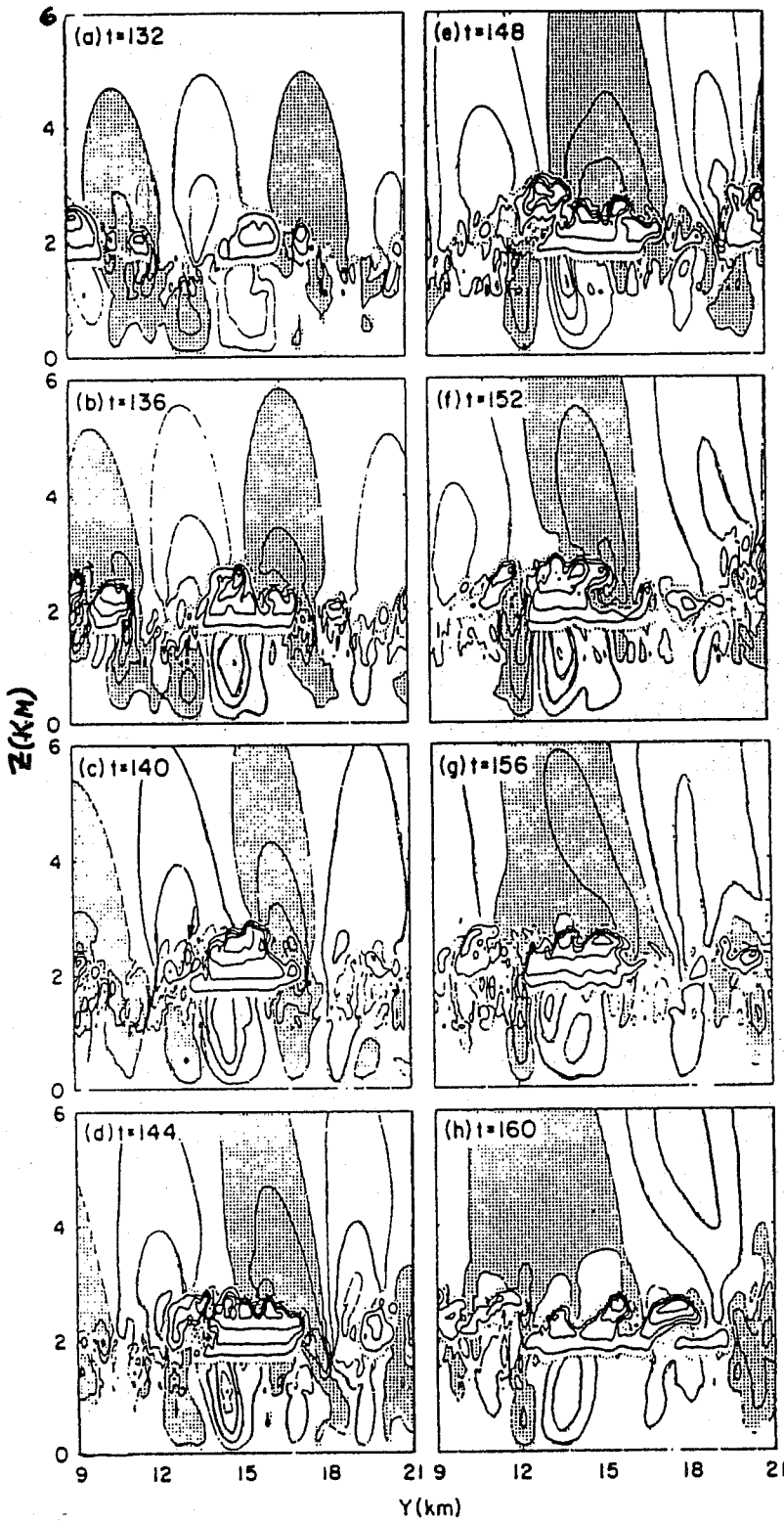

Fig. 6 Plots of w and q_c for the strong shear case of Clark et al. (1986). Contour interval of w is 1 m s^{-1} and q_c is .2 g kg^{-1}. Only odd values of w are shown.

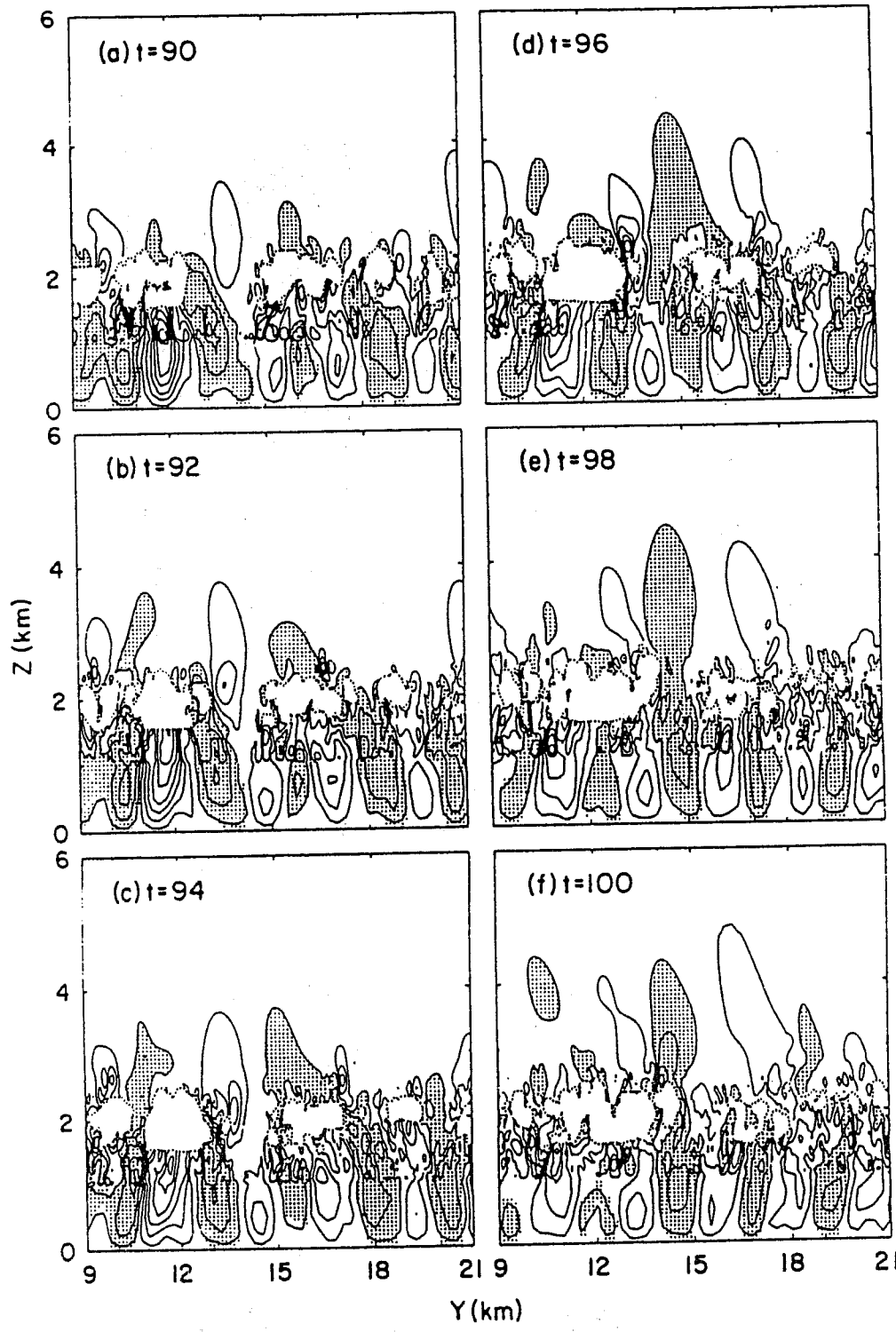

Fig. 7 Same as Fig. 6 except for moderate shear case. Contour interval of w is .5ms^{-1}.

v) Three dimensional simulations

Hauf and Clark (1989) ran a case similar to the strong speed shear case of Clark et al. (1986) using a three–dimensional model. Power spectra analysis of their results indicated deep modes similar to those found in the two–dimensional experiments except

that the deep modes were quite three–dimensional in character. Figure 8 shows the time evolution of the power spectra of w from one of their three–dimensional moist experiments. The t = 200 min results show a significant fraction of energy is in the wave field at similar horizontal wavenumbers as the boundary layer eddies.

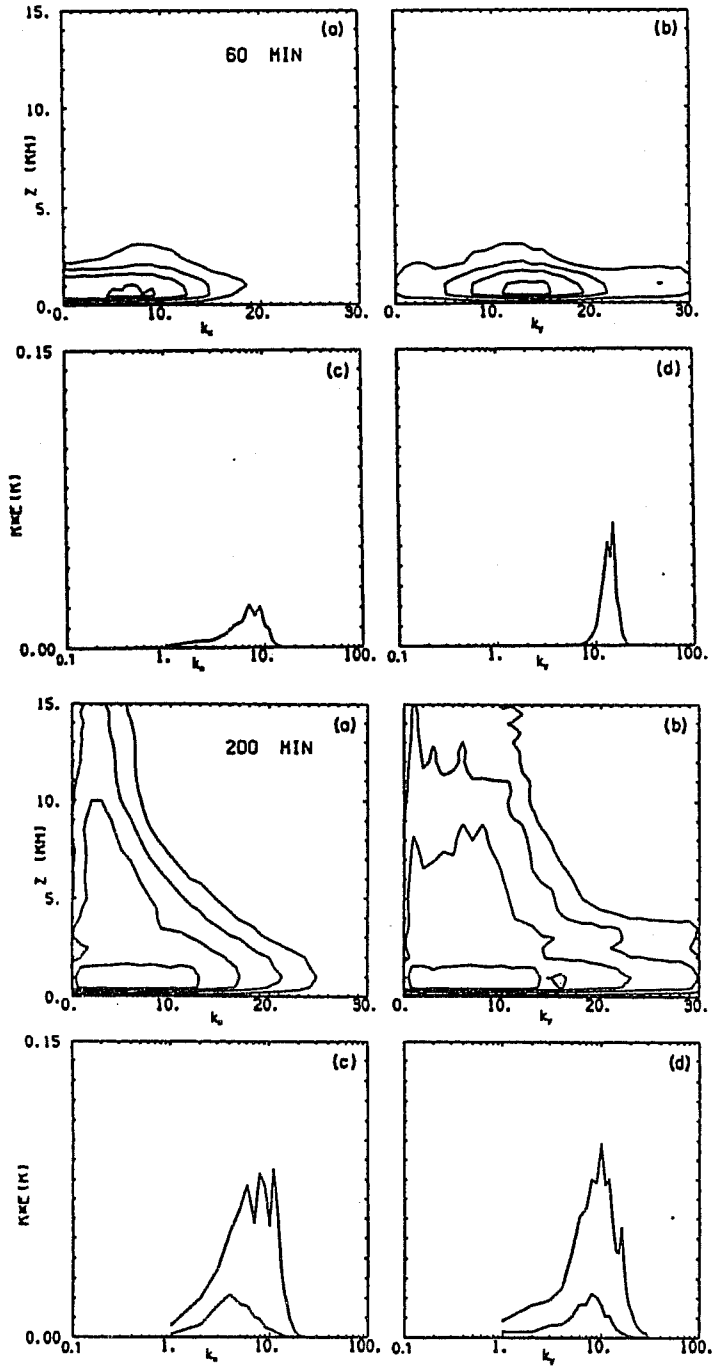

Fig. 8 Power spectra of w at t= 60 and 200 min from the moist experiment ST-M of Hauf and Clark (1989). As in Fig. 4 both height dependance and one-dimensional energy content are shown in $x-$ and $y-$ direction. The bottom curve in the 1–D spectra are for energy between z = 3 and 15 km (waves) and upper curve for z = 0 to 15 km (waves and eddies).

One serious problem with their results was that the model simulations did not have a balanced large scale flow. The intial structures of shear were quickly mixed out by boundary layer processes since the baroclinic and other forces responsible for the presence of the background shear had not been considered in their model framework. Some attempts at including baroclinic forces in an *ad hoc* manner resulted in shear maintenance and a commensurate increase in thermally forced gravity waves. Inclusion of moisture resulted in a scattered field of clouds with the overall power spectra of w similar to the dry runs.

One of the results of using speed shear in three–dimensions is that the modal structure tends to be broken in nature. Gravity waves like to align normal to the shear whereas boundary layer eddies like to align parallel with the shear when the atmospheric layers are considered in isolation. For deep modes spanning the two layers a broken structure appears to be one possible long time solution structure. Sufficient directional shear (90^0 turning) does not present this type of conflict between the two layers and banded structures are then possible within both layers for the deep modes.

3. SIMULATIONS OF PRECIPITATING CUMULUS

i) Severe thunderstorm simulations

Balaji and Clark (1988) simulated the initiation and subsequent evolution of a severe thunderstorm for the CCOPE day of 1 August 1981 using the wind field shown in the hodograph in Fig. 9. The simulation started with a heated unstable boundary layer and evolved through a number of natural stages of convection. The first stage was the development of boundary layer eddies which then excited overlying gravity waves. The deep modes associated with the eddies and waves eventually initiated cumulus clouds which over time evolved into cumulocongestus and finally into a multi–cellular storm. The simulation was not successful in getting beyond the multi–cellular stage into a super cell stage primarily because the simulation finally ran out of moisture in the boundary layer.

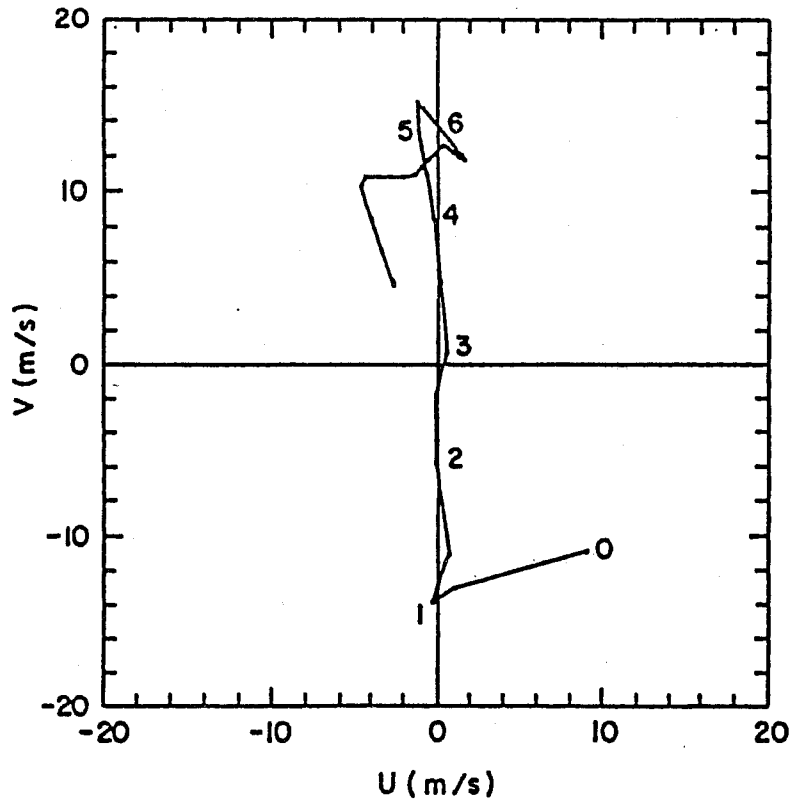

Fig. 9 Wind profile for 1 August 1981. Numbers indicate height in km. Galilean transformation and rotation has been applied to original data. (From Balaji and Clark, 1988)

This last effect was an artifact of using cyclic boundary conditions in order to stay within the *near field* of the thermal forcing and at the same time having a rather limited domain of only 60 by 60 km in the horizontal.

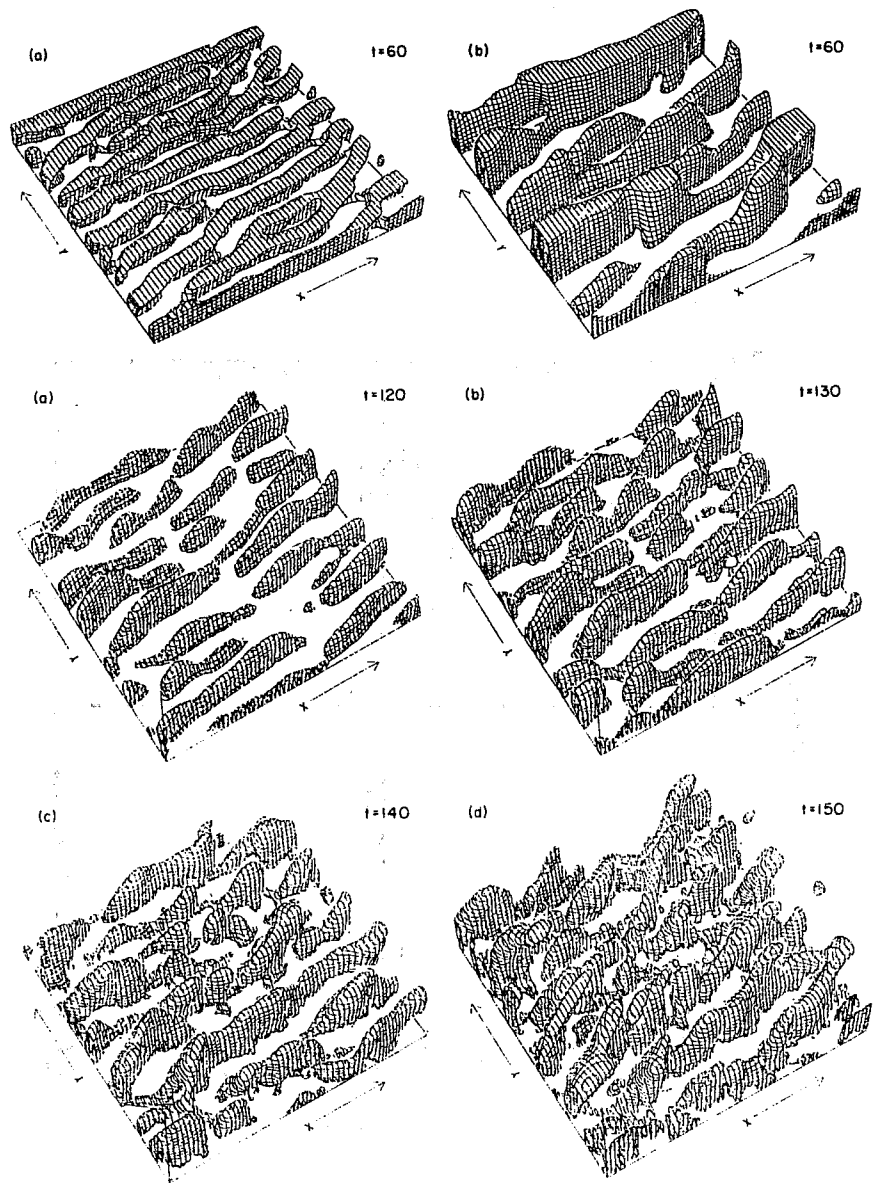

Fig. 10 w at t = 60 min from linear model run and at t ≥ 120 min from nonlinear model. For linear model region of w ≥ 1 mm s^{-1} is shown and for nonlinear model regions of w ≥ .5 m s^{-1} are shown.

A persistent mean shear profile was obtained in this simulation by the rather ad hoc procedure of using an unusually large value of surface friction which tied the surface wind to its observed value. Without this or some equivalent procedure the boundary layer eddies would have mixed out the shear and shut down any interesting convection development.

There was good agreement between the initial modal structures from the linear

and nonlinear models as shown in Fig. 10. The nature of the modal response was the development of boundary layer rolls aligned with the boundary layer shear with bands of overlying gravity waves aligned normal to the shear near the top of the boundary layer. The waves were also aligned parallel to the more widely spaced boundary layer rolls which was possible because of the directional shear. Plots of modal amplitude versus time, as shown in Fig. 11, showed that the modes saturated at about two hours into the calculations. The relative growth rates between the Rayleigh and deep modes was similar prior to this time for the linear and nonlinear models.

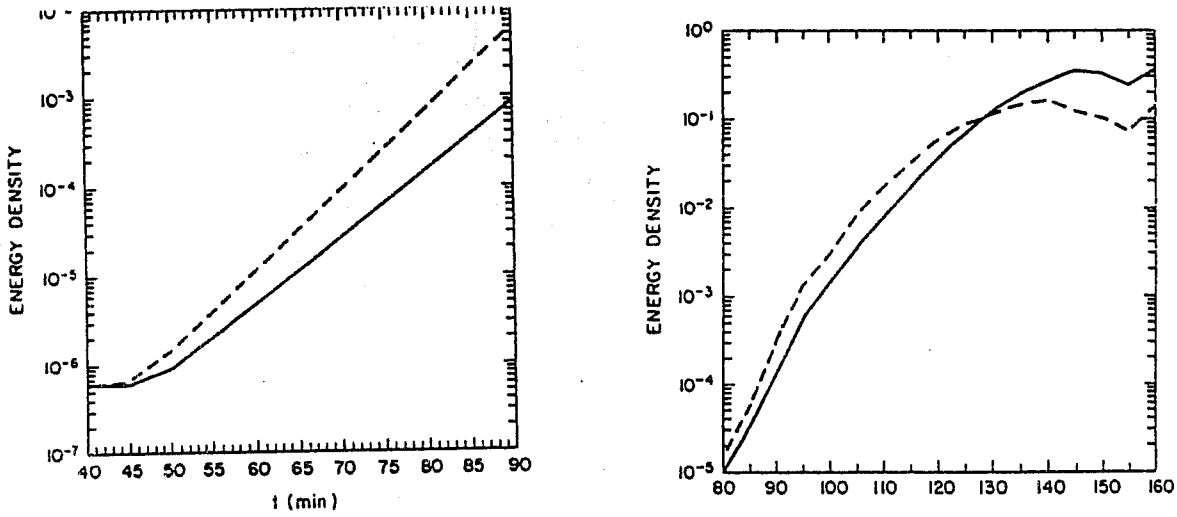

Fig. 11 Growth histories for two dominant modes from Balaji and Clark (1988). (a) is from the linear model and (b) from the nonlinear model. The solid line represents the deep mode (k_x, k_y= 0,5) and the dashed line the Rayleigh mode (k_x, k_y=0,9).

One of the interesting results of these experiments was the appearance of a recurrence time of enhanced cloud development. The relative motion between the overlying gravity wave field and the clouds which are tied to the boundary layer eddies resulted in a period of enhanced cloud growth. When the updrafts of the wave field and cloud updrafts are most highly correlated then maximal enhanced cloud growth can occur. This period was about one hour for these calculations. This effect is shown in Fig. 12 which shows contours of maximum w against t and z.

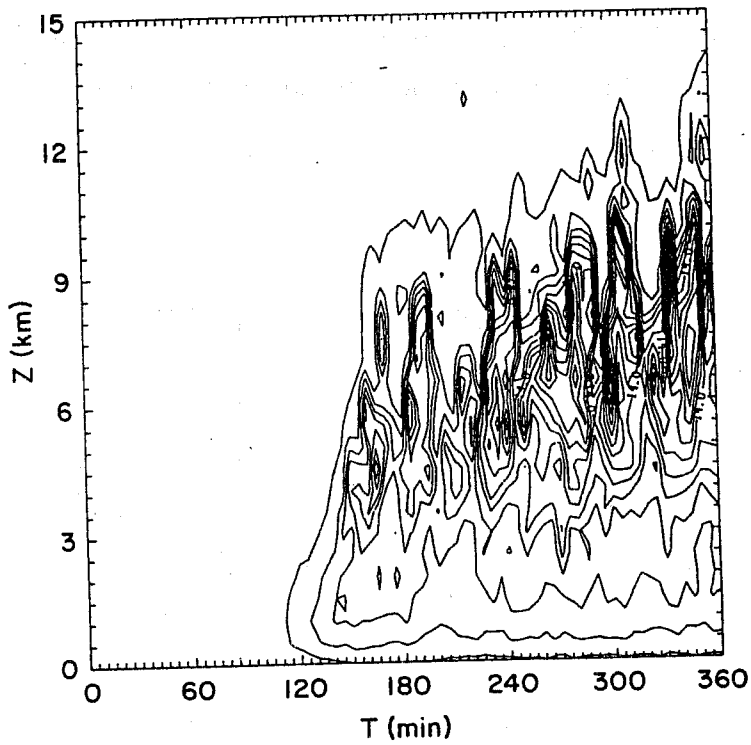

Fig. 12 Plots of w_{max} against t and z. Contour interval is 2. m s^{-1}.

Another interesting result of these calculations was the development of discrete propagation within the severe multi–cellular storm resulting from new cell development on the existing deep modes. Discrete propagation as a result of gust front dynamics was not a possibility within these calculations as no rain reached the surface. The time scale of new cell generation was about 10–13 min which is in good agreement with the observational period of about 15 min of such phenomenon by Chalon et al. (1976). The model of Wilhelmson and Chen (1982) which relied upon gust front dynamics for their new cell regeneration obtained a period of 30 min. The general character of the multi–cellular storm produced in the Balaji and Clark simulations is shown in Fig. 13.

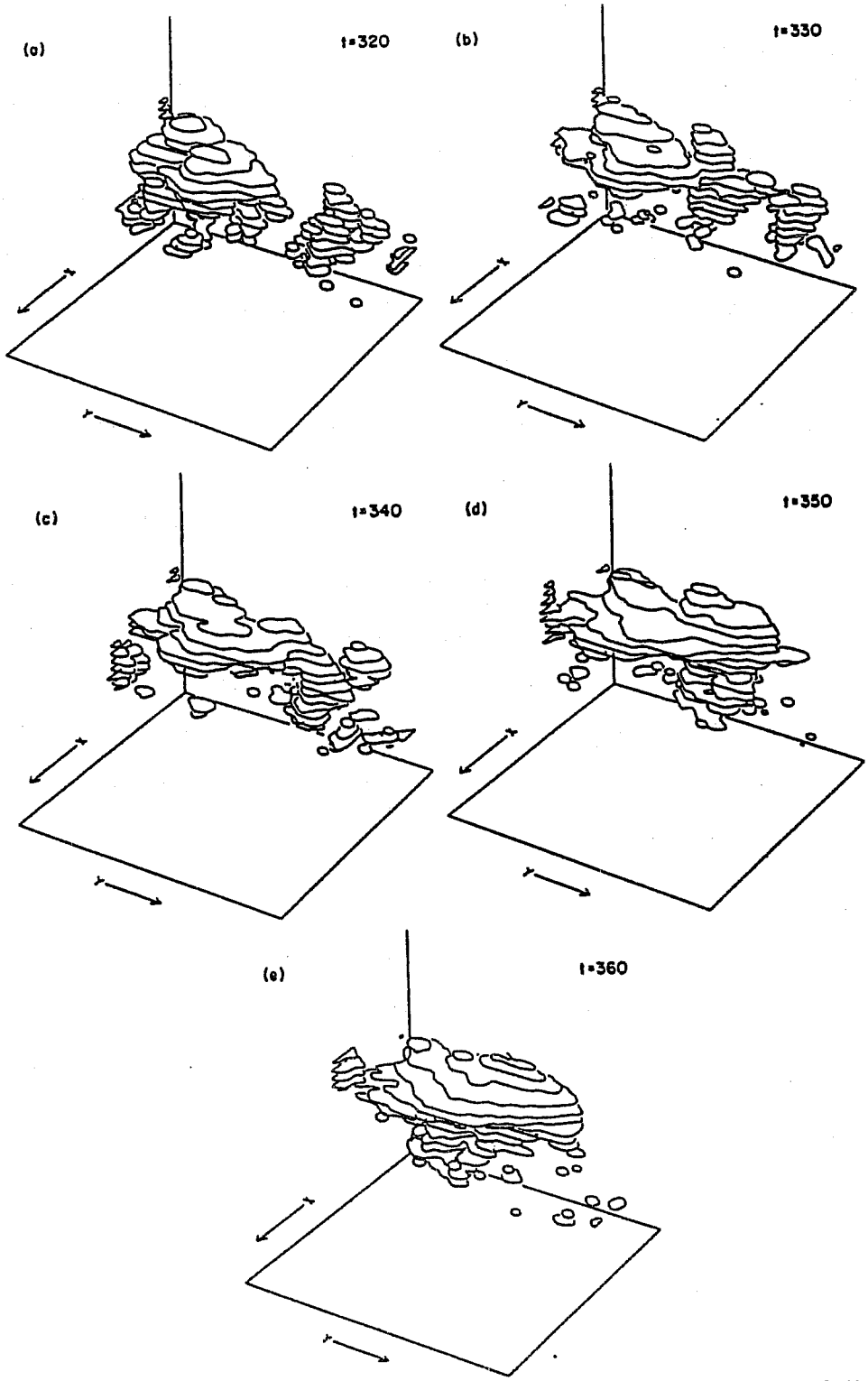

Fig. 13 Aerial views of cloud field from t =320 to 360 min from Balaji and Clark (1988). Contour encloses region of $q_c > .01$ *g* kg^{-1}.

ii) Larger domain simulations over gently sloping terrain

In the previous three-dimensional simulations described, ad hoc procedures had to be used to maintain any sort of balanced outer scale of motion within which the convection could develop. To circumvent this problem Redelsperger and Clark (1990) considered the evolution of convection over gently sloping terrain where the combination of differential heating and Coriolis effects were sufficient to maintain interesting profiles of spanning level shear. Their simulations also assumed some background shear in the initial geostrophic zonal flow. These simulations were run with and without moisture.

There was a large variability across the domain of the spanning level shear structure. In particular, the western slope had much less shear than the eastern slope because on the eastern slope the differential heating tended to compliment the background shear. As a result only very weak convection developed on the western slope as compared with the eastern slope. On the eastern slope the character of the convection ranged from banded to scattered depending upon the degree of directional shear near the top of the boundary layer. Figure 14 shows a comparison between the character of the eastern and western slope convection for a dry run having a background shear of $5 \times 10^{-3} s^{-1}$ over the first 5.5 km of height.

For the dry runs the horizontal scale selection of the gravity waves showed some interesting doubling effects at later times. Figure 15 shows power spectra of w for two of the dry experiments from Redelsperger and Clark. Note the $k = 14$ mode which has developed in DRY3A between 1:10 and 2:40 pm.

An interesting speculation which arises as a result of these experiments involves a possible temporal dependence on the modal selection of moist convection. When the clouds become established prior to the scale doubling effect as seen in the dry experiments then this scale doubling does not occur in the moist simulations. The clouds appear to lock onto the existing scales provided by the dry dynamics. The speculation then is if the onset of significant cloudiness had occurred later in time would their horizontal scale selection have again mimicked the dry case and shown a much larger range in horizontal scale? Fig. 16 shows the power spectra for the moist experiment WETA from Redelsperger and Clark.

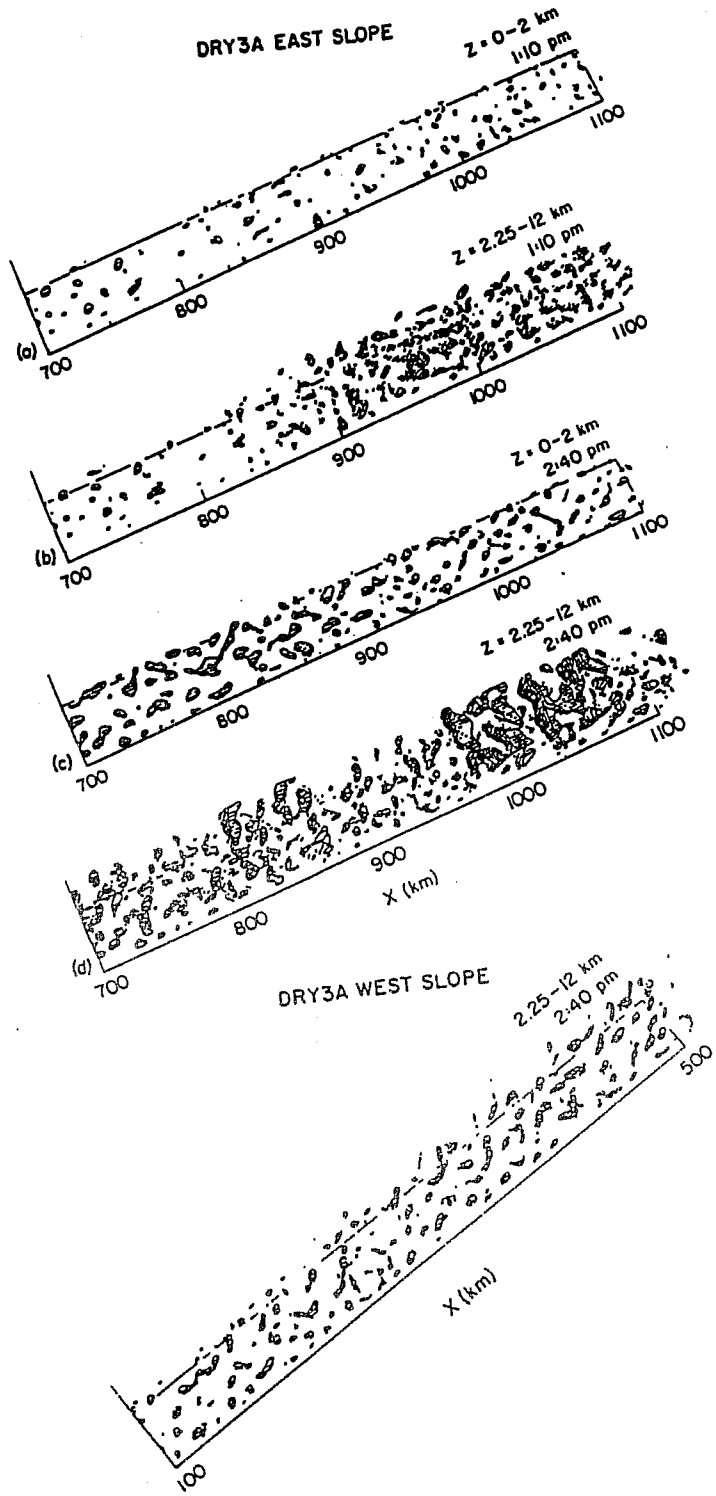

Fig. 14 Perspective views of w on eastern plain at t = 1:10 and 2:40 pm for the boundary layer and free atmospheric regions. The western plain is also shown but only at t= 2:40 pm for the western plain.

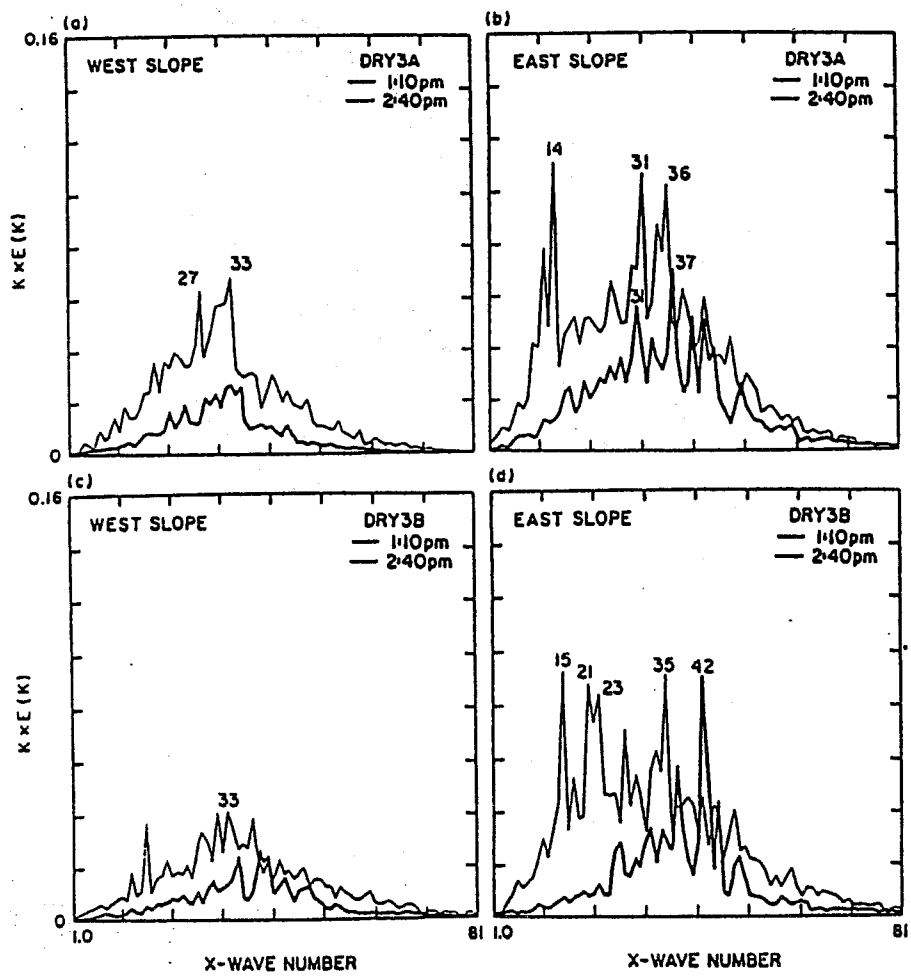

Fig. 15 Power spectra of w from two of the three-dimensional dry experiments of Redelsperger and Clark (1990). DRY3A used a background shear of $5 \times 10^{-3}\ s^{-1}$ *and DRY3B* $3 \times 10^{-3}\ s^{-1}$.

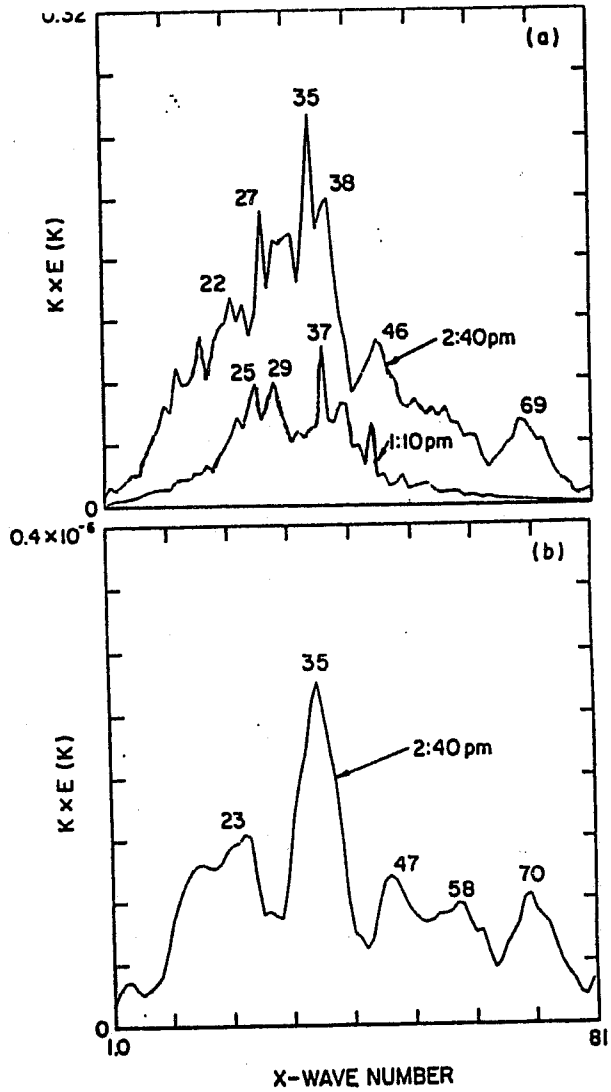

Fig. 16 Power spectra of w and q_c for the eastern slope for the three-dimensional experiment WETA from Redelsperger and Clark (1990) for t = 1:10 and 2:40 pm. k=1 refers to λ_x = 400 km.

iii) Denver convergence line simulations of moist convection

Crook et al. (1991) present simulations of airflow over an isolated mountain which is an idealization of the Palmer lake divide in Colorado. The outer scale structure of the flow within which the convection develops results as a response to surface heating and the convergence zone in the lee which is a result of stable airflow over/around the mountain. Fig. 17 shows the general character of the flow for the unheated and heated regimes, respectively. The convergence zone is clearly depicted by the linear zone of vertical vorticity caused by tilting of horizontal vorticity. The onset of boundary layer eddies and thermally forced gravity waves makes the picture rather chaotic looking by comparison.

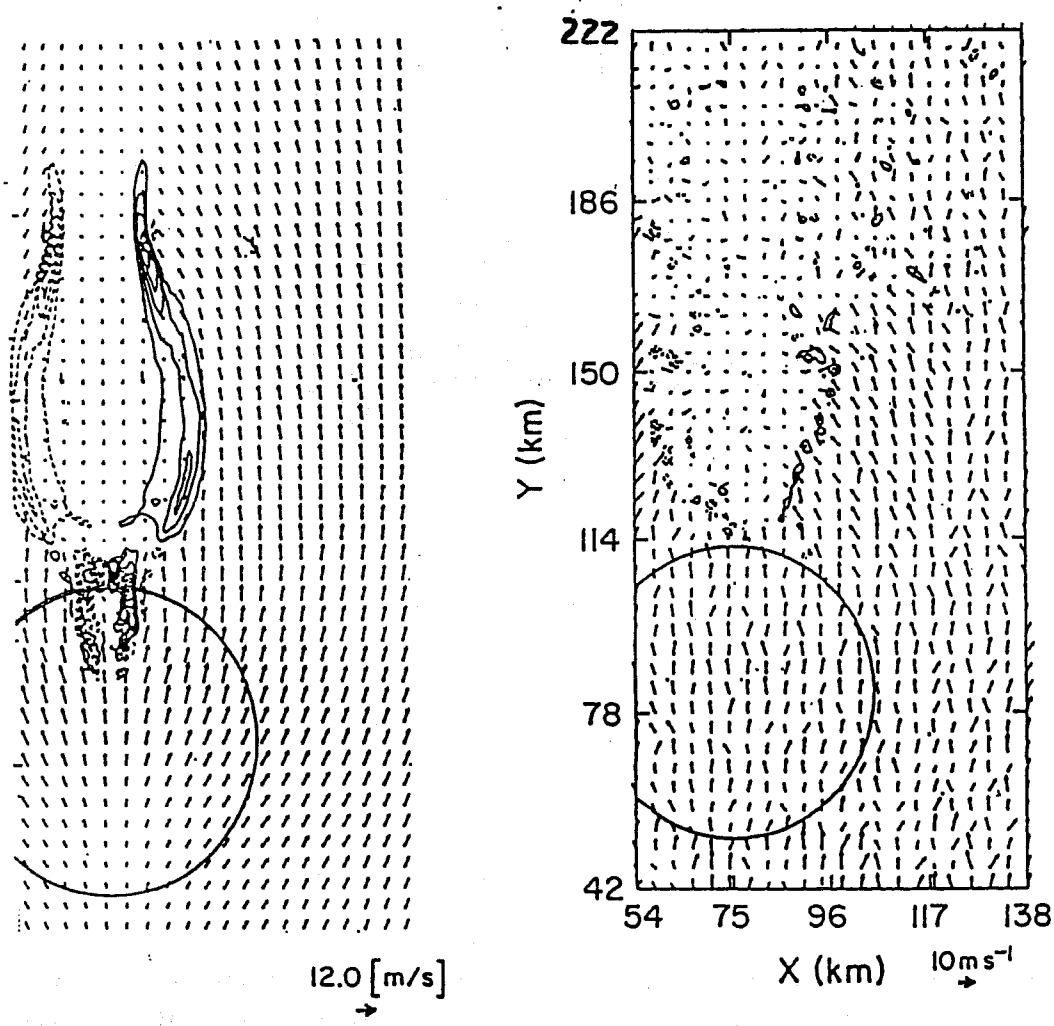

Fig. 17 Horizontal velocity and vertical vorticity, ζ, from Crook et al. (1991). Contour interval of ζ is 5×10^{-4} s^{-1}. (a) corresponds to t = 400 min prior to any heating and (b) corresponds to t = 840 min which is approximately 400 min after thermal heating was turned on.

Clouds develop along the convergence zone where relatively weak tornadoes are frequently spawned. Local bands of clouds are observed to form along the convergence line and they are typically oriented at a substantial angle to the the convergence line. Their horizontal spacing is being about $\approx$ 10 km. The simulations of Crook et al. (1991) show a similar type of cloud structure evolving as a result of thermally forced gravity wave response. Figure 18 shows plots of the shear produced by the heating and plots of w at z= 4.5 km within the window region marked in the shear diagram.

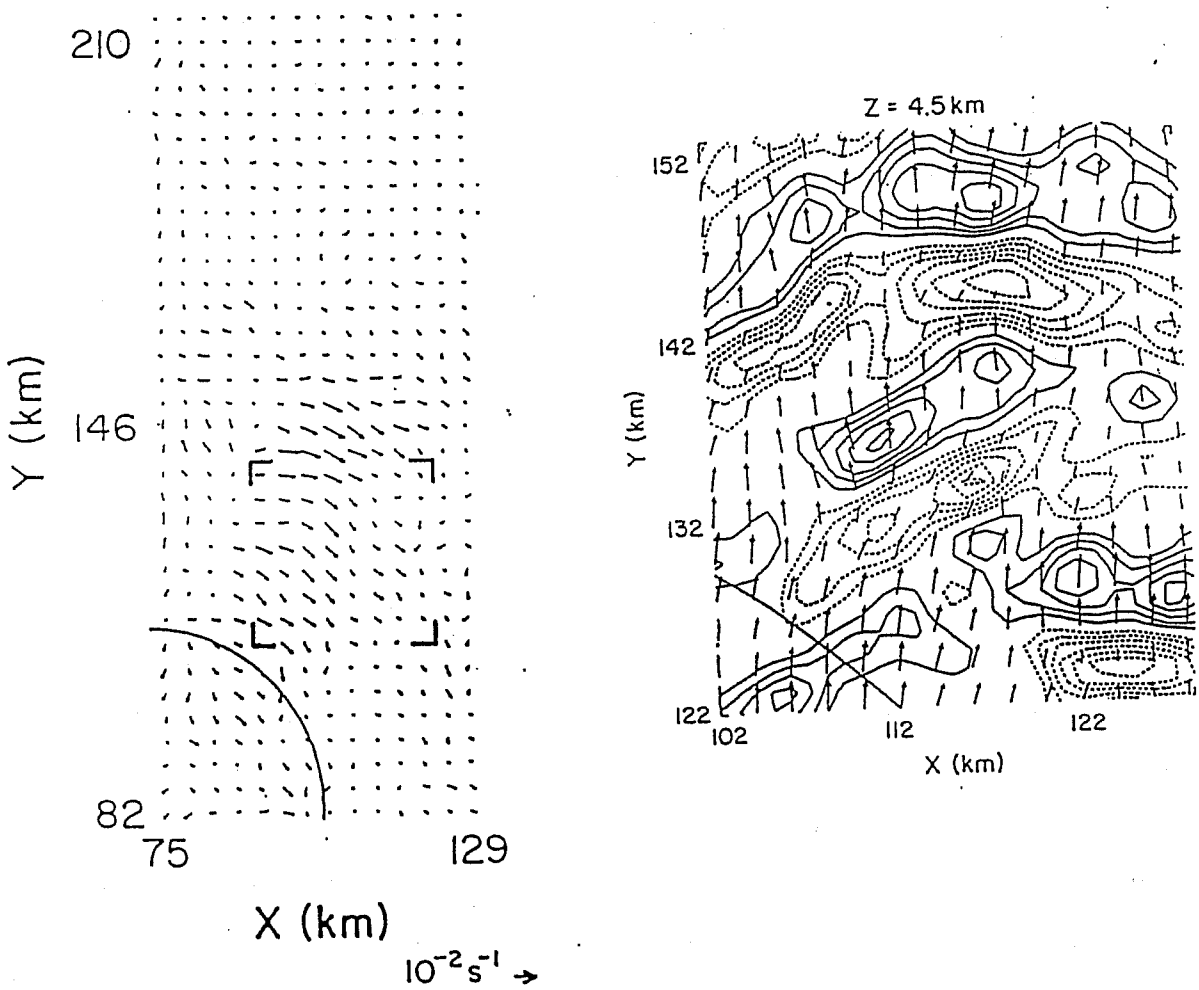

Fig. 18 Vertical shear of the horizontal wind at the midlevel of the boundary layer (1 km AGL) (a) and vertical velocity at 4.5 km AGL (b). Contour interval in (b) is .2 ms^{-1}.

4. CONCLUSIONS

The type of results presented suggest that further investigation on the role played by the dominant forced deep modes in organizing convection is warranted. Perhaps they could be used to help define some of the parameter space necessary to categorize cloud fields. More information on the nature of the tuning is required. Is the weak type of resonance inherently non–hydrostatic? This question could be easily addressed using a linear model.

To obtain an indication of whether or not this deep mode characteristic is active in fine scale population studies one could simply vary the treatment of gravity waves

within a case study, i.e. with and without a radiation condition. Are the statistics of the population study sensitive to such effects? If so, then this would suggest that gravity waves play an important organizing role.

The cases presented so far had significant shear near the top of the boundary layer which acts to couple some of the boundary layer eddies with overlying gravity waves. Is this type of shear structure always necessary for such modes to exist? If so, then how frequent is its occurance? A more thorough analysis of and comparison between the linear and nonlinear results seems necessary.

As noted in a number of the simulations presented the results can be plagued by the difficulty of treating both the outer scale within which the convection develops and the convective scales themselves. The mechanisms which lead to a balance (at least on the time scale of the convection) of the outer scale need to be rather carefully considered in such three-dimensional simulations. On longer term simulations this becomes particularly important when radiative/convective equilibrium is being considered. For example in such cases, the simple assumption of constant heat flux, $F_\uparrow$, is certainly inappropriate. The assumption of $F_\uparrow = C_d(\theta - \theta_{sfc})$ is likely to give a different equilibrium state as it allows freedom for the convection to chose its own equilibrium state. Similar arguments hold for moisture and momentum fluxes.

REFERENCES

Balaji, V. and T. L. Clark, 1988: Scale selection in locally forced convective fields and the initiation of deep cumulus. *J. Atmos. Sci.*, **45**, 3188–3211.

Chalon, J.-P., J.C. Fankhauser and P.J. Eccles, 1976: Structure of an evolving hailstorm. part I: General characteristics and cellular structure. *Mon. Wea. Rev.*, **104**, 564–575.

Clark, T.L., 1979: Numerical simulations with a three-dimensional cloud model: lateral boundary condition experiments and multi-cellular severe storm simulations. *J. Atmos. Sci.*, **36**, 2191 – 2215.

Clark, T. L., and T. Hauf, 1986: Upshear cumulus development: A result of boundary layer/free atmosphere interactions. Proceedings, 23rd Conf. on Cloud Physics, Snowmass, Colorado. Proceedings, 23rd Conf. on Cloud Physics, Snowmass, Colorado.

Clark, Terry L., Thomas Hauf, and Joachim J. Kuettner, 1986: Convectively forced internal gravity waves: Results from two–dimensional numerical experiments.

Quart. J. Roy. Meteor. Soc.,**112**, 899-925

Crook, N. Andrew, Terry L. Clark, and Mitchell W. Moncrieff, 1991: A numerical study of the denver cyclone Part II. Interaction with the convective boundary layer. *J. Atmos. Sci.*, (accepted)

Hauf, T. and T. L. Clark, 1989: Three dimensional numerical experiments on convectively forced internal gravity waves. *Q.J. Roy. Meteor. Soc.*, **115**, 309-333.

Hill, G.E., 1974: Factors controlling the size and spacing of cumulus clouds as revealed by numerical experiments. *J. Atmos. Sci.*, **31**, 646 – 673.

Hill, G.E., 1977: Initiation mechanisms and development of cumulus convection. *J. Atmos. Sci.*, **34**, 1934 – 1941.

Kuettner, J. P., P. A. Hildebrand, and T. L. Clark, 1987: Convection waves: Observations of gravity wave systems over convectively active boundary layers. *Quart. J. Roy. Meteor. Soc.*,**113**, 445-467

Ley, B.E. and W.R. Peltier, 1981: Propagating mesoscale cloud bands. *J. Atmos. Sci.*, **38**, 1206–1219.

Mason, P. J., and R. I. Sykes, 1982: A two–dimensional numerical study of horizontal roll vortices. *Quart. J. Roy. Meteor. Soc.*, **108**, 801–823.

Miller, M.J., 1978: The Hampstead storm: A Numerical simulation of a quasi-stationary cumulonimbus system. *Quart. J. Roy. Meteor. Soc.*, **104**, 413–427.

Redelsperger, J.-L. and Terry L. Clark, 1990: On the initiation and horizontal scale selection of convection over gently sloping terrain. *J. Atmos. Sci.*, **47**, pp. 516-541.

Schlesinger, R.E. 1978: A three–dimensional numerical model of an isolated thunderstorm: Part I. Comparative experiments for variable ambient wind shear. *J. Atmos. Sci.*, **35**, 690–713.

Wilhelmson, R.B. and J.B. Klemp, 1978: A numerical study of storm splitting that leads to long lived storms. *J. Atmos. Sci.*, **35**, 1974–1986.

Wilhelmson, R.B. and C.-S. Chen 1982: A simulation of the development of successive cells along a cold outflow boundary. *J. Atmos. Sci.*, **39**, 1466–1483.

Xu, K.-M. and S.K. Kreuger, 1991: Evaluation of cloudiness parameterizations using a cumulus ensemble model. *Mon. Wea. Rev.*, **119**, 342–367.

Yau, M.-K. and R. Michaud, 1982: Numerical simulation of a cumulus ensemble in three dimensions. *J. Atmos. Sci.*, **39**, 1062 – 1079.